A Numerical Approach to Investigate the Impact of Acid Asphaltene Sludge Formation on Wormholing During Carbonate Acidizing

DOI:
10.1115/1.4051738

Document Version
Accepted author manuscript

Journal of Energy Resources Technology JUNE 2022, Vol. 144 / 063001-1

DOI: 10.1115/1.4051738

A Numerical Approach to Investigate the Impact of Acid-Asphaltene Sludge Formation on Wormholing During Carbonate Acidizing

Ilyas Khurshid[1]
Khalifa University, Abu Dhabi, P.O. Box 12277, United Arab Emirates
ilyas.khushid@ku.ac.ae

Emad W. Al-Shalabi
Khalifa University, Abu Dhabi, P.O. Box 12277, United Arab Emirates
emad.walshalabi@ku.ac.ae

Imran Afgan
Khalifa University, Abu Dhabi, P.O. Box 12277, United Arab Emirates
University of Manchester, Manchester, M13 9PL, United Kingdom
imran.afgan@ku.ac.ae

Hazim Al-Attar
UAE University, Al Ain, UAE
hazim.alattar@uaeu.ac.ae

ABSTRACT

Carbonate acidization is the process of creating wormholes by injecting acid to increase reservoir permeability and oil production. Nevertheless, some reservoir oils are problematic with low asphaltene stability, which affects the wormholing process. The interactions between acid, rock, and asphaltene lead to acid-asphaltene sludge formation, which reduces oil productivity and acid injectivity. Neglecting this sludge formation, leads to over predicting the depth of the wormhole penetration. Therefore, a numerical model was developed in this study to provide a better understanding of acid-asphaltene sludge formation effect on wormhole creation and propagation in carbonates. A 1D radial model was developed by coupling fluid flow equations in porous media with asphaltene deposition and acid-asphaltene reactions. Then, the developed model was validated and utilized to investigate the effects of different parameters on wormholing including asphaltene presence, acid injection volume and concentration, formation temperature and porosity, and asphaltene concentration. Results showed that acid injection in carbonates with asphaltenic-oils reduces wormhole penetration from 40% to total pore blockage as opposed to reservoirs without asphaltene deposition. The findings also highlighted that shallow wormhole penetration is more pronounced with high volume of acid injection, high porous formations, less diluted acid, and high concentration of asphaltene. In addition, there is an optimum acid injection volume at which wormhole penetration is high and its infiltration is deep into the formation. This is the first work to discuss modeling of acid-asphaltene sludge formation and subsequent wormhole development in carbonates, which is particularly important for problematic crude oils.

Keywords

Wormholing; Asphaltene Deposition; Acid Injection; Acid-Asphaltene Sludge; Irreversible Formation Damage

[1] Ilyas Khurshid.

INTRODUCTION

Chemical reactions in porous media between rock and different injected fluids is of interest in many subsurface geochemical processes including CO_2 sequestration, low salinity water injection, polymer injection, surfactant injection, microbial injection, and production enhancement by hydraulic fracturing and acidizing [1-6]. Both experimental and numerical studies play an important role in evaluating the environmental effects and economic viability of these techniques [7, 8]. The implementation of these techniques, especially the acid injection in carbonates, is complex and challenging. During acid injection in carbonate rocks and particularly limestones, the surface reaction rates are high and thus, the transfer of mass restricts the net reaction rate, originating highly non-uniform and branched dissolution pathways known as wormholes [9, 10].

A lot of work has been done over the years on the thermal hydraulics and computational efforts in general, [11-31]. However, advanced techniques for reactive transport modelling have only recently started to receive the requisite attention. For example, in [32-35] experimental data was used for model development, validation and penetration of wormholes. The knowledge of these wormholes and their penetration aids have been utilized in determining the effect of acidization on skin factor in the context of improved oil recovery. The development of wormholes could be a consequence of carbon dioxide (CO_2) based enhanced oil recovery (EOR). In CO_2 based EOR operations, millions of cubic feet of anthropogenic CO_2 is injected in the reservoirs as opposed to only hundreds of cubic feet of acid is injected in an acid job for stimulation [34]. Moreover, in CO_2 based EOR operations, the injected CO_2 might create a weak acid (carbonic acid) while in acid stimulation, very strong acids such as hydrochloric and hydrofluoric acids are injected. The latter renders the estimation of wormhole in acid stimulation operations more critical compared to CO_2 based EOR. Therefore, it is crucial to understand and determine the safety, success, and economic feasibility of oil recovery in highly reactive operations such as acidization.

In carbonate reservoirs, acidization is usually conducted by injecting concentrated acid into the formation to enhance permeability and consequently, oil production. In these reservoirs, acid injection at low rates creates shallow and thick wormholes, while injection at high rates creates branched wormholes

with shallow penetration. Nevertheless, at optimum injection rate, deep and extended wormholes might be created with least amount of acid [36]. Consequently, several researchers proposed global acidization models [10, 37-40]. These models could determine the amount of acid needed for creating wormhole and could predict the wormhole propagation rate around the wellbore. However, these models ignored the effect of asphaltene presence on wormholing in the porous media. Although in practical acidizing treatments, a solvent preflush is used to dissolve asphaltenes, this paper addresses the cases when preflush could not dissolve all of the asphaltenes leading to an irreversible formation damage.

In acid injection operations, acid-oil interaction is an aspect that has received limited attention in wormhole creation and propagation. During an acid job, when the acid interacts with the asphaltenic crudes, the acid might cause instability of dissolved asphaltene leading to asphaltene deposition [41, 42]. Consequently, the reaction of the injected acid with asphaltene might form a black and sticky substance in the reservoir, which is known as acid-asphaltene sludge. This material enhances gravity segregation due to its density and forms a layer of acid-asphaltene sludge in the reservoir. Thus, decreasing reservoir permeability and at worse conditions it might completely shut off production. Moreover, in most of the laboratory studies, the wormholing experiments are usually performed in single phase, water-saturated conditions, which do not allow capturing sludge formation [43-45].

Houchin et al. [46] performed a number of tests and reported that acid induced asphaltene sludge is formed for crude oils with API gravities $\geq$ 27 ^{o}API and asphaltene concentration $\leq$ 3 wt. %, and this sludge is more severe for reservoirs under secondary and tertiary recovery activities. Kumar et al. [47] studied the effect of phase saturation on wormholing and showed that it has a significant impact on the acid operation [26]. They experimentally determined an optimum acid injection rate 10 cm^3/min with minimum branching in the fully water saturated cores. Whereas for the fully oil saturated cores, the optimum acid injection rate was reported at 5 cm^3/min. They also found no optimum rate for waterflooded residual oil cores. However, they ignored the acid-asphaltene reactions, acid-asphaltene sludge formation, and its effects on wormholing process. Similarly, AlMubarak et al. [48] investigated the acid-induced emulsion and the precipitation of asphaltene in low permeability reservoir and they found that acid systems are not compatible with several oils when they interact with each other.

Furui et al. [38] observed a mismatch in predicting wormhole formation during matrix acidizing between theoretically and conventionally developed models as opposed to field data [41]. This observation was based on performing inverse analysis on wormholing data from horizontal and inclined wells in oil and gas fields from Middle East and North Sea. The discrepancy is due to investigating acid-rock reaction and acid-asphaltene reactions separately. Several researchers considered acid-rock reactions while ignored acid-asphaltene reactions [1, 37, 38]. However, Rietjens and Van Haasterecht considered acid-asphaltene reactions and ignored acid-rock reactions [49]. Moreover, Alrashidi et al. [50] analyzed the effect of bio-oil dispersants on asphaltene sludge during acidization and they found that the dispersant could decrease the formation of asphaltene sludge formation. Thus, both aspects of acid-rock and acid-asphaltene reactions need to be studied and further investigated. Nevertheless, in order to understand asphaltene effect during acidization and acid-asphaltene sludge formation, several factors need to be investigated which affect asphaltene deposition, acid-asphaltene reaction, and acid-asphaltene sludge formation.

Therefore, in this study, the experimental data of the above sources [43-48] in the literature were used to propose a model, which considers simultaneous acid-rock and acid-asphaltene reactions as well as acid-asphaltene sludge formation. Furthermore, the effect of several factors on wormholing was investigated in both presence and absence of asphaltene slug formation. These factors include presence of asphaltene, acid injection volume, formation temperature, formation porosity, acid concentration, and asphaltene concentration. To the best of our knowledge, there are no published works focusing on modeling acid-asphaltene sludge formation and its subsequent wormhole development. This paper aims at providing a better understanding of the effects of asphaltene deposition and acid-asphaltene sludge formation on wormhole creation and propagation in carbonates.

NUMERICAL MODEL DEVELOPMENT

In this study, reactive transport modeling of sludge formation during acidization was performed by considering the Darcy scale model at two-phase conditions. The model is based on combining single-phase reactive, advective, and dispersive transport in the porous media with deposited asphaltene as a solid phase. This technique has the ability to capture comprehensive picture of the interplay of the mechanisms

of asphaltene deposition, acid-asphaltene reaction, and acid-asphaltene sludge formation. These phenomena will aid in determining the critical rate of wormhole generation around the wellbore for maximum permeability enhancement. Figure 1 shows the flowchart followed for asphaltene based wormhole penetration modeling describing how the study is conducted. The 1D developed model incorporates the rock-acid-asphaltene interactions in the following sequence: i) deposition of asphaltene ii) diffusion of acid in the immediate wellbore vicinity of rock-asphaltene interface, iii) Surface reaction at the asphaltene-formation interface between the acid and asphaltene, iv) formation of acid-asphaltene sludge deposits on the rock surface and its diffusion away from the interface.

Figure 2 shows the mathematical description of the developed model for asphaltene based wormhole penetration modeling. In this study, it was assumed that light and heavy oil components are produced, the oil residue (asphaltene) is deposited in the reservoir, capillary and gravity forces are negligible, and the temperature of the reservoir is constant during acid injection.

Fluid Flow in Porous Media. The single-phase model is extended to a two-phase formulation for fluid flow in porous media. Thus, Darcy's law is used, as it is the fundamental equation for fluid-flow in porous media where the phase flow is given by:

$$\frac{\partial \phi}{\partial t} + \nabla . v_t = 0, \tag{1}$$

where ϕ is formation porosity, t is time, and v_t is velocity of all the phases present in the porous media including water and oil.

The acid-rock surface reaction rate could be determined by calculating acid mass transfer from the bulk acid-water solution to the rock surface. This technique helps in finding the sequential rate of acid concentration on the rock surface interface from the bulk acid-water solution. Therefore, the rate of mass transfer from the bulk solution to the rock surface interface could be determined as:

$$F_r = k_m (C_{ac} - C_{rf}), \tag{2}$$

where F_r is the rate of bulk fluid mass transfer from the bulk fluid to the rock surface interface, k_m is the mass transfer-coefficient, C_{ac} is concentration of acid in the aqueous phase, and C_{rf} is concentration of acid at rock-fluid interface.

Asphaltene Deposition Model. Among different organic matters present in the crude oil, asphaltenes are the most complex mixture of colloidal suspended molecular particles with no certain chemical formula [50]. Consequently, due to different aggregate sizes, asphaltenes have a wide range of molecular weights from 1,650-500,000 g/mol [52]. To study the behavior of precipitation and deposition of asphaltene during production and other enhanced oil recovery operation, the asphaltene onset pressure is the most important factor. This onset pressure is determined by using a mixture of reservoir fluids at varying percentage of injected fluid in the reservoir. However, this technique only addresses the static asphaltene behavior and thus, the risk of asphaltene deposition under dynamic conditions is ignored.

To encounter this issue, dynamic asphaltene behavior is used to have a clear picture of asphaltene deposition in oil recovery operations. Thus, dynamic behavior shows that when asphaltene deposits in the pores of the reservoir, the reservoir fluid loses its heavy components. This process causes a reverse phenomenon where the density of live oil increases and that of dead oil decreases. In a giant oil field in the Middle East, the density of dead oil was 0.805 g/cm^3 and that of the produced oil was in the range of 0.83-0.84 g/cm^3 [53]. This reverse-density phenomenon indicates that with the continuous oil production and associated reservoir pressure drop, the equilibrium of reservoir fluids is disturbed and due to gravity segregation, the heavy oil component (asphaltene) is deposited in the reservoir. The risk of asphaltene deposition is even more severe in case of light crudes, when the reservoir fluids are in a highly under-saturated reservoir pressure [41]. When acid is injected in the porous media, its flow is described by the continuity equation as follows:

$$\frac{\partial}{\partial t}\left(S_l \rho_{as} X_{as} \phi + S_l \rho_l w_{as} \phi\right) = -\left(\rho_{as} \frac{\partial V_{as}}{\partial t} + \frac{\partial}{\partial r}\left(\rho_l w_{asp} v_l + \rho_l w_{as} v_l\right)\right). \tag{3}$$

where S is saturation in fraction, ρ is density in kg/m^3, X is asphaltene concentration, ϕ is porosity in fraction, v is fluid flow in m/s, w is mole concentration, V is deposited concentration, and t is time in s. Subscripts *a, o, l, g, as,* and *asp* refer to aqueous, oil, liquid, gas, asphaltene, and suspended asphaltene, respectively. One should note that further details can be found in Appendix A.

For asphaltene deposition, several researchers have performed experimental and simulation studies to determine the risk of asphaltene deposition. Gruesback and Collins observed that the deposition

of asphaltene is dependent on the concentration of asphaltene in the reservoir fluid [54]. Thus, they derived a simple model by considering a single-phase flow. Wang and Civan [55] considered some complexities and showed that asphaltene deposition is controlled by its concentration in the reservoir fluid, deposition behavior, trapping, and plugging mechanism in the porous media. They mentioned that the observed plugging of the pore throat is related to asphaltene concentration, liquid saturation, superficial velocity, and gravity segregation. They derived the following equation:

$$\frac{\partial \eta_{as}}{\partial t} + (v_l - v_{cr.l}) d_{as} \beta_{as} = S_l \alpha_{as} C_{as} \phi + S_l \gamma v_l C_{as} \,, \tag{4}$$

where η_{as} is deposition rate of asphaltene, v_l is interstitial velocity, d_{as} is asphaltene deposition rate, β_{as} is asphaltene entrainment rate coefficient, S_l is saturation of liquid, α_{as} is coefficient of asphaltene surface deposition, γ is plugging coefficient, and C_{as} is asphaltene concentration. Therefore, the precipitation and deposition of asphaltene on porous rock surfaces could lead to severe formation damage, pore blockage, and reservoir relative permeability impairment [56]. The deposition of asphaltene on a rock surface is controlled by two mechanisms; mass transfer and chemical reactions for flocs appearance, precipitation, and deposition of asphaltene. Afra et al. mentioned that during CO_2 injection, the injected CO_2 reacts with the amine functional group of asphaltene [57]. This reaction decreases the stability of asphaltene in the oil and thus, asphaltene could be destabilized through physical interactions and chemical reactions.

Soulgani et al. performed several experiments for asphaltene deposition and observed the deposition of asphaltene decreased as soon the injected fluid velocity is increased [58]. This phenomenon shows that mass transfer is a less controlling mechanism. It was also found that when temperature increases, the heat transfer coefficient decreases at a higher rate, which promotes asphaltene deposition. This behavior of asphaltene shows that asphaltene deposition is controlled by temperature of the system. Therefore, chemical reaction is the determining mechanism of asphaltene deposition. A number of researchers developed different models and investigated asphaltene [58-62]. However, it was found that the deposition of asphaltene is controlled by chemical interactions of injected fluid and oil. Therefore, in this work, the deposition of asphaltene in the porous media was estimated by the asphaltene deposition model in Equation (5) and was added with Equation (4) to estimate the net asphaltene deposition volume

fraction that will deposit in the reservoir. Different coefficients for asphaltene deposition could be found in Table 1.

$$\frac{\partial \omega_{as}}{\partial t} = K \frac{C_{as}}{v} e^{-E/RT}, \quad (5)$$

where ω is rate of asphaltene deposition per unit time, χ is reaction rate coefficient, *C* is concentration, *E is* activation energy, R is universal gas constant, T is reservoir temperature, and *v* is acid flow rate. The subscript "*as"* stands for asphaltene.

Capturing Changes in Porosity and Permeability. After the deposition of asphaltene, the reservoir rock surface area will be modified. This deposition would decrease the reservoir permeability. Thus, changes in reservoir permeability were captured in the model through updating reservoir porosity and the related permeability using the following equations [62]:

$$\phi = \phi_i(1 - S_{as}), \quad (6)$$

$$\frac{k}{k_i} = \left(\frac{\phi}{\phi_i}\right)^e \left(\frac{1-\phi_i}{1-\phi}\right)^2, \quad (7)$$

where *k* is reservoir permeability, ϕ is reservoir porosity, S is saturation, and subscripts *i* and *as* represent the initial stage and asphaltene, respectively. The exponent *e* with values of 3, 5, and 12 represent clean formations, anhydrite precipitation, and for coreflooding experiments showing the technical time scale for anhydrite dissolution and precipitation, respectively. It should be noted that an *e* value of 3 was used in this work. This is because of the assumption that the carbonate formation is clean without clay, which is usually the case. In addition, it was assumed that the rock is 100% calcite in this study and the effects of dissolution/precipitation of other solid species were not considered as it requires a comprehensive geochemical engine.

Sludge Formation Model. After acid injection, insoluble organic precipitate, known as acid-asphaltene sludge, is formed [49]. This sludge is too sticky and is highly undesirable type of formation damage, which could adversely affect the whole acid job. The formed acid-asphaltene flocs has the tendency to form acid-asphaltene aggregates leading to the formation of acid-asphaltene sludge. This is due to the charged groups present on asphaltene boundary, which demonstrates the sticky mass of sludge formed at the acid-

asphaltene interface. It was assumed that the formation of sludge will hinder the direct contact of acid with the rock. Thus, the acid transfer from the aqueous phase to the solid asphalt phase is described by [49]:

$$\omega_{as} + HC_{aq} \underset{k_{-1}}{\overset{k_1}{\rightleftarrows}} \omega H^+ C_{as}^- , \tag{8}$$

where HC represents acid, subscript "aq" stands for aqueous, "k" coefficient is phase transport, and $XH^+C_{as}^-$ is the formed acid-asphaltene sludge term abbreviated as Y_{as} and is represented by:

$$\omega H^+ C_{as}^- \underset{k_{-2}}{\overset{k_2}{\rightleftarrows}} Y_{as} . \tag{9}$$

After combining Equations (8) and (9), the rate of acid-asphaltene sludge formation is given by:

$$\frac{dY_{as}}{dt} = k_2[\omega H^+ C_{as}^-] - k_{-2}[Y]_{as}. \tag{10}$$

The concentration of acid is also considered constant at a certain time and it increases with acid injection. Thus, the boundary condition for acid-asphaltene sludge formed at initial time (t is zero) is given by:

$$\frac{dY_{as}}{dt} = k_1 \omega_{as} HC_{aq} V. \tag{11}$$

Modified Wormhole Propagation Model. Based on Equation (11), the rate of acid-asphaltene sludge formation is proportional to the concentration of phase transport by asphaltene, the acid activity in aqueous phase, and its volume. Economides et al. assumed that for wormholing, the injected acid would dissolve a certain volume of rock to penetrate in the formation [9]. They used this approach to determine the acid volume to predict the distance of wormhole penetration. It was observed that the dissolution of small rock fragments will form few wormholes while the dissolution of large rock fraction will create more branched and deep wormholes in the rock matrix. They proposed an equation for rock acidization by injected acid as follows [9]:

$$r_{wo} = \sqrt{r_r + \frac{N_c V}{\pi \phi h \tau}} , \tag{12}$$

where r_{wo} is radial wormhole penetration in feet, r_r is wellbore radius in feet, N_c is acid capacity number that is defined by the ratio of amount of rock mineral dissolved by the injected acid to the amount of rock mineral present in a unit rock volume, V is the acid volume in cubic feet, h is the reservoir height in feet, and τ is wormholing efficiency that is estimated from coreflooding. The wormholing efficiency depends on

acid capacity number and number of acid pore volume injected until breakthrough [10]. However, this model has a couple of constraints; it overlooks fluid loss, reaction with organic matter present in crude oil, and asphaltene deposition in the porous media. Ignoring these factors over predicts the depth of wormhole penetration. Equation (13) is the proposed modified model, which was derived by deducting Equation (11) from Equation (12) to formulate the net reaction of acid-asphaltene sludge formation that will occur in the reservoir.

$$r_{wo} = \sqrt{r_r + \frac{N_c V - k_1 \omega_{as} HC_{aq} V}{\pi \phi h \tau}}. \quad (13)$$

Table 1 provides the values of the different variables used in this study. The data for wormholing efficiency and its propagation with strong acid in core samples were taken from Furui et al. [38]. The rock is carbonate and the acid is hydrochloric acid as mentioned by Furui et al. [38]. Economides et al. mentioned that the wormhole efficiency can be estimated from the data of a linear coreflooding, and is given by [1]:

$$\tau = N_c \times PV, \quad (14)$$

where PV is the pore volume of the acid injected at the time of wormhole breakthrough at the end of the core. In order to determine the rate of acid-asphaltene sludge formation in the initial stage of reaction, the concentration of asphaltene was assumed to be constant and the reverse reactions in Equations (8) and (9) were neglected. The objective of this study is to evaluate the effect of organic matter present in reservoir oil on wormholing, by combining acid-formation reaction and acid-organic matter reaction to the formation of acid-asphaltene sludge. Figure 3 shows a graphical representation of acidization with and without asphaltene, creation of acid-asphaltene sludge, and aggregation of sludge to acid-asphaltene sludge in the porous media.

During the development of the acid-asphaltene sludge model, the main objective is to define formation damage. Unfortunately, very limited experimental research is conducted on wormholing in asphaltene deposited cores. Nevertheless, Kumar et al. [47] investigated acidization of both brine saturated and residual oil saturated cores as shown in Figures 4 (i) and (ii), respectively. The findings of Kumar et al. [47] showed that the organic layer acts as a physical wall or barrier between acid and rock and thus, validates the concept/technique presented in this paper. Therefore, the results generated are more realistic

where the formation of acid-asphaltene sludge reduces acid-rock reaction and further hinders wormhole penetration. As was previously mentioned, this fundamental fact is usually ignored leading to large discrepancies between simulation and field data [38].

DEVELOPED MODEL VALIDATION. In modeling acid-asphaltene sludge formation, it was observed that the most difficult part is to model the deposition of asphaltene. This is because in acidization, the injected acid is usually very strong and it will definitely react, but determining asphaltene deposition is complex. Asphaltene deposition is controlled by rock properties, formation water composition, oil properties, thermodynamic conditions of the reservoir, and flow rate of the injected fluids. To validate the developed numerical model, the experimental work conducted by Soulgani et al. [58] was used. In the latter experimental work, the authors used coreflooding to determine the formation damage caused by asphaltene deposition. The details of experimental run are given in Table 1**.**

Figure 5 presents a good match between the experimental data and our simulation results. One should note that the observed asphaltene deposition has adverse effects on formation permeability and acid is usually injected to recover this permeability. It is evident from Figure 5 that with the increase in injected pore volumes, the formation damage increases. The formation damage is presented by the permeability ratio of altered to initial permeability. Furthermore, one can observe from the latter figure that due to asphaltene deposition, the reservoir permeability decreased by 46%. This decrease will certainly have a negative effect on oil production from a reservoir. Moreover, data from experiments conducted by different researchers were used to further evaluate the accuracy of the developed model. Figure 6 shows a good match with Bagheri et al. [63]. In the latter study, the authors performed experimental investigation of asphaltene precipitation and deposition process during different production schemes such as natural depletion, lean gas injection, and CO_2 injection. The simulation results of this work were compared with their CO_2 injection case because CO_2 forms a weak acid in the reservoir by mixing with formation water. More details about their experimental work are described elsewhere [63]. Further explanation on the asphaltene deposition and acid-asphaltene sludge formation will be discussed in the results and discussion section.

RESULTS AND DISCUSSION

After validation against the experimental data, the developed model was utilized to predict the deposition of asphaltene, asphaltene-acid reaction, and acid-asphaltene sludge formation. The important factors affecting wormholing that were thoroughly investigated in this work include the presence of asphaltene, acid injection volume, formation temperature, formation porosity, acid concentration, and asphaltene concentration. Typical values of these parameters were selected in the base case run, which represent typical carbonate reservoir conditions. Table 1 shows the values of these parameters used in this study. The effect of each parameter on the wormholing process is described below.

ASPHALTENE EFFECT. Figure 7 shows the effect of asphaltene presence on wormhole penetration. This figure shows that wormhole penetration in the presence of asphaltene is slower as opposed to the absence of asphaltene. In the latter figure, the wormhole penetration after 100 gal/ft of acid injection is approximately 2.75 ft. Nevertheless, when asphaltene is present, the relationship between wormhole penetration and volume of injected acid shows an extremely low penetration that is less than 1 ft after injecting the same amount of acid (100 gal/ft). It is worth mentioning that a monotonic increase in wormhole penetration is observed with acid injection in the absence of asphaltene. However, when asphaltene is present in the crude oil, the wormhole penetrates just 1 ft with acid injection of 40 gal/ft and with further acid injection, the penetration rate decreases. The reason behind this decrease in wormhole penetration is the presence of asphaltene as well as formation and deposition of acid-asphaltene sludge. Thus, the injected acid could not directly react with the rock matrix.

The acid first reacts with asphaltene, forming acid-asphaltene sludge where most of the injected acid is consumed, regardless of the acid injection rate. Consequently, injecting acid in reservoirs with asphaltenic crudes could lead to severe formation damage near the wellbore as evident from Figure 7. This formation damage, caused by acid-asphaltene sludge, decreases the wellbore production and might sometimes shut-off oil production. Therefore, acid induced asphaltene sludge will adversely affect the effectiveness of wormholing.

ACID INJECTION VOLUME EFFECT. The effect of acid injection volume on wormholing can also be deduced from Figure 7. The latter figure was produced using an acid injection at a certain acid concentration of 15%

by weight and asphaltene concentration that is limited to just 1 percent in the reservoir. From Figure 7, it is evident that the wormhole penetrated deep in the formation when 40 gallons of acid was injected and afterwards the penetration decreased. These 40 gallons of acid could be considered as an optimum acid volume at which the wormhole propagation is high with minimum sludge formation. This is supported by the increase of wormholing depth with increasing injected acid volume up to 40 gallons. Afterwards, any further increase in injected acid volume results in a decrease in wormhole penetration.

These findings were not observed by Daccord et al. [9], Hung et al. [32], Buijse and Glasbergen [37], and Furui et al. [38]. Because they ignored the presence of asphaltene and acid-asphaltene sludge formation and considered that the wormhole propagation is proportional only to the rate of acid injection. Hung et al. model [10] considered the wormhole propagation is linear while Daccord et al. model [9] showed it depends on the average wormhole velocity. Moreover, both studies of Buijse and Glasbergen [37] and Furui et al. [38] studies incorporated the linear relationship between acid injection rate and wormhole propagation. Therefore, it is important to consider the effect of asphaltene presence in porous media during wormholing; as the study shows that after a certain acid injection volume, enormous acid-asphaltene sludge forms, which leads to severe formation damage and low penetration of wormhole.

TEMPERATURE EFFECT. The effect of temperature on wormholing in the presence of asphaltene was determined as depicted in Figure 8. The latter figure mimics reservoirs with different depths of 1000, 1800, 2600, 3400, and 4200 meters that correspond to reservoir temperatures of 40, 60, 80, 100, and 120 °C, respectively. It is evident that the rate of wormhole penetration is high in the shallow reservoirs, which is due to the exothermic reaction nature of carbonate dissolution process. The low temperature of a reservoir favors dissolution reaction and results in high acid solubility. Therefore, wormholing phenomenon slows down at high temperatures. Regarding the precipitation of dissolved particles, it is evident that when the temperature of a reservoir is high, the process of wormholing will be low and the dissolved particles will remain soluble in the media. Figure 8 illustrates that wormholing by acid injection in the presence of asphaltene will be better in shallow reservoirs as opposed to deep reservoirs. Nevertheless, one should carefully consider the dissolutions in the near wellbore region, which might sometimes lead to casing failure and wellbore stability problems.

FORMATION POROSITY EFFECT. The sensitivity of formation porosity on wormholing in the presence of asphaltene is shown in Figure 9. In high porous formations, the surface area of contact between acid and rock surfaces is large, and the wormholing process is expected to develop more effectively than in low porosity formations. However, in the presence of asphaltene, a reverse phenomenon occurs. This is because acid will form acid-asphaltene sludge instead of moving deeper in the formation as shown in Figure 9. This sludge might coagulate together to create a mat of acid-asphaltene sludge as shown in Figure 3 and it will block acid penetration and reservoir pores/pathways. Therefore, the continuous injection of acid will dissolve more rock minerals only in the near wellbore region, creating vugs around the wellbore as shown in Figure 3, and the pressure drop over the acid invaded region decreases significantly.

Consequently, further volumes of injected acid removes some sludge and it might divert and force acid flow to enter smaller pores that might give rise to the branching phenomenon. However, this branching prohibits further growth of deep penetrating single-wormholes. The branching phenomenon is usually intensified at higher injection volumes of acid, which might explain the start of the decreasing trend at 100 gal/ft of acid injection volume for the 30% porosity curve in Figure 9. In addition, it is evident from Figure 9 that for the same volume of acid injection, the wormhole penetration is deeper for low porous formations than in high porous formations. It is clear from the figure that after injecting 100 gal/ft of acid, the 10% porosity scenario shows 2.5 ft of wormhole penetration, while the 30% porosity scenario shows less than 1 ft of wormhole penetration. This behavior highlights that the shallow wormhole penetration is more pronounced in high porous formations than low porous formations. One should note that these observations hold under the assumptions of no direct acid-rock reaction, which is expected to increase the formation porosity.

ACID CONCENTRATION EFFECT. Figure 10 illustrates the effect of acid concentration on wormhole penetration. The acid might be injected in the reservoir in a number of forms such as regular acid, foamed acid, and emulsified acid. These different forms might have some benefits such as foamed acid provides good leak-off control and emulsified acid might have deep penetration. However, regular acid gives better results at higher flow rates [47]. Therefore, a regular acid injection was utilized at different concentrations of hydrochloric acid including 10, 20, and 30 percent.

The results showed that in the presence of asphaltene, the increase in acid concentration causes a shallower wormhole penetration. This is supported from the latter figure where high acid concentration (30 percent) results in wormhole penetration of just 0.5 ft. However, a 10 percent acid solution results in wormhole penetration of more than 3 ft at an acid injection of 100 gal/ft. The reason behind this low penetration at high acid concentration is that the high acid concentration promotes sludge formation.

ASPHALTENE CONCENTRATION EFFECT. The effect of asphaltene concentration in reservoir fluid on wormholing is presented in Figure 11. During acid injection, the reaction of acid with asphaltene depends on its mixing, concentration, and solubility with the asphaltene. It could be observed from Figure 11 that when asphaltene concentration is low, this creates less acid-asphaltene sludge and hence, the acid penetrates deeper into the formation. This is supported by the case of 0.5 percent asphaltene (shallow wormhole penetration). Moreover, the negative penetration shown in Figure 10 illustrates total pore blockage by acid-asphaltene sludge formation and deposition, which halted further acid penetration as supported by the case with just 1.5 percent asphaltene. Therefore, when the concentration of asphaltene is high, the amount of acid-asphaltene sludge formation increases, and the penetration of acid in the formation decreases. These phenomena will lead to severe and irreversible formation damage.

SUMMARY AND CONCLUSIONS

A numerical 1D model was successfully developed in this study to predict acid-asphaltene sludge formation and its effect on wormholing during acid treatment in carbonates with asphaltenic oils. The main findings of this work can be summarized as follows:

- The study shows for the first time that the injection of acid in carbonates with asphaltenic-oils results in sludge formation that reduces the wormhole penetration from 40 percent to total pore blockage as opposed to reservoirs without asphaltene deposition.
- The effectiveness of wormholing process is worsen by sludge formation, which was found to be highly dependent on reservoir porosity, acid concentration, and solubility of asphaltene in acid.

- Shallow wormhole penetration is more pronounced in high porous formations, with less diluted acid, and in the presence of high concentration of asphaltene. The wormholing penetration is intensified by increased volume of acid injection.
- There is an optimum acid injection volume at which wormhole penetration is high and its infiltration is deep into the formation.
- It is recommended to better characterize the properties of reservoir fluid before an acid treatment job as the effectiveness of wormholing is controlled by asphaltene concentration.

This is the first work to discuss modeling of acid-asphaltene sludge formation and subsequent wormhole development in carbonates, which is particularly important for problematic crude oils. In the future work, the proposed model will be expanded to 2D and 3D, which enables capturing the branching phenomenon and further validating the model against CT scan images for the wormhole.

ACKNOWLEDGEMENTS

The authors wish to acknowledge Khalifa University of Science and Technology in Abu Dhabi, UAE for providing the computational and research facilities.

APPENDIX A

The flow characteristics of oil, gas, and aqueous phases are presented by the fluid flow continuity equations as follows:

$$\frac{\partial(\rho_o w_o S_o \phi)}{\partial t} = -\frac{\partial(\rho_o w_o v_o)}{\partial r} \quad \text{(A-1)}$$

$$\frac{\partial(\rho_g w_g S_g \phi)}{\partial t} = -\frac{\partial(\rho_g w_g v_g)}{\partial r} \quad \text{(A-2)}$$

$$\frac{\partial(\rho_a w_a S_a \phi)}{\partial t} = -\frac{\partial(\rho_a w_a v_a)}{\partial r} \quad \text{(A-3)}$$

Combining Equations (A-1) to (A-3) gives:

$$\frac{\partial}{\partial t}\left(\rho_o w_o S_o \phi + \rho_g w_g S_g \phi + \rho_a w_a S_a \phi\right) = -\frac{\partial}{\partial r}\left(\rho_o w_o v_o + \rho_g w_g v_g + \rho_a w_a v_a\right) \quad \text{(A-4)}$$

For acid component, if we neglect the diffusion, the above-derived equations are given by:

$$\frac{\partial}{\partial t}\left(\rho_o \omega_{w,o} S_o w_o \phi + \rho_g \omega_{w,g} S_g w_g \phi + \rho_a \omega_{w,a} S_a w_a \phi\right) = -\frac{\partial}{\partial r}\left(\rho_o \omega_{w,o} w_o v_o + \rho_g \omega_{w,g} w_g v_g + \rho_a \omega_{w,a} w_a v_a\right) \quad \text{(A-5)}$$

For simplification, we assumed the acid injection rate is constant. Thus, Equation (A-5) becomes:

$$\frac{\partial}{\partial t}\left(\rho_o \omega_{w,o} w_o S_o + \rho_g \omega_{w,g} w_g S_g + \rho_a \omega_{w,a} w_a S_a\right) = -\frac{q_{inj}}{\phi}\frac{\partial}{\partial r}\left(\rho_o \omega_{w,o} w_o v_o + \rho_g \omega_{w,g} w_g v_g + \rho_a \omega_{w,a} w_a v_a\right). \quad \text{(A-6)}$$

Therefore, during acid injection, the mass balance equation for asphaltene deposition is:

$$\frac{\partial}{\partial t}\left(S_l \rho_{as} X_{as} \phi + S_l \rho_l w_{as} \phi\right) = -\left(\rho_{as}\frac{\partial V_{as}}{\partial t} + \frac{\partial}{\partial r}\left(\rho_l w_{asp} v_l + \rho_l w_{as} v_l\right)\right) \quad \text{(A-7)}$$

where S is saturation in fraction, ρ is density in kg/m^3, X is asphaltene concentration, ϕ is porosity in fraction, v is fluid flow in m/s, w is mole concentration, V is deposited concentration, and t is time in s. Subscripts *a, o, l, g, as,* and *asp* refer to aqueous, oil, liquid, gas, asphaltene, and suspended asphaltene, respectively.

NOMENCLATURE

Symbols

A	*Area of porous media, meter-square*
C	*Concentration, percentage*
D	*Coefficient of diffusion*
d	*Deposition rate, 1/t*
E	*Energy for activation, J/mol*
F	*Coefficient of drag force*
h	*Reservoir height, m*
K	*Coefficient of reaction rate*
k	*Mass transfer coefficient*
L	*Pores Length, m*
R	*Universal gas constant, J/mol.K*
r	*Pore radius, m*
S	*Saturation, %*
T	*Reservoir temperature, K*
V	*Volume, m^3*
v	*Fluid velocity, m/s*
Y	*Rate of sludge formation, 1/t*

Greek Letters

ϕ	*Formation porosity, %*
w	*Mole concentration*
ρ	*Density, kg/m^3*
α	*Surface deposition coefficient*
β	*Entrainment rate coefficient*
γ	*Plugging deposition rate coefficient*
τ	*Wormholing efficiency, %*
χ	*Reaction rate coefficient*
η	*Net deposition, 1/t*
ω	*Rate of asphaltene deposition per unit time*

Subscripts

a	*aqueous*
ac	*acid*
as	*asphaltene*
c	*carbonate*
e	*exponent*
g	*gas*
i	*initial*
l	*liquid*
o	*oil*
r	*reservoir*
s	*suspension*

REFERENCES

[1] Economides, M.J., Hill, A. D., Ehlig-Economides, Zhu, D. 2013. "Petroleum Production Systems". Pearson Education.

[2] Khurshid, I., Choe, J. 2015. "Analysis of Asphaltene Deposition, Carbonate Precipitation, and their Cementation in Depleted Reservoirs during CO_2 Injection". Green hou. Gases Sci. Techn. 5, 1-11.

[3] Islam, A., Sun, A., Lu, J. 2016. "Simulating In-Zone Chemistry Changes from Injection Time to Longer Periods of CO2 Storage". Environ. Earth Sci. 75, 1346.

[4] Khurshid, I., Fujii, Y. 2021. "Geomechanical analysis of formation deformation and permeability enhancement due to low-temperature CO_2 injection in subsurface oil reservoirs". J. Petrol. Explor. Prod. Tech. 11, 1915:1923.

[5] Na, J., Xu, T., Jiang, Z., Bao, X., Yongdong, W., Feng, B. 2016. "A Study on the Interaction of Mud Acid with Rock for Chemical Stimulation in an Enhanced Geothermal System". Environ. Earth Sci. 75, 1–13.

[6] Al-Shalabi, E.W., Sepehrnoori, K. 2017. "Low Salinity and Engineered Water Injection for Sandstone and Carbonate Reservoirs". Gulf Professional Publishing, Elsevier, 1st Edition, Cambridge, MA, USA.

[7] Vikram, R., Rob, K. 2017. "Sustainable Shale Oil and Gas". Chapter 6-Potential for Liquid Contamination of Groundwater, Sustainable Shale Oil and Gas, Elsevier.

[8] Ejeh, C., Afgan, I., AlMansob, H., Brantson, E., Fekala, J., Odiator, M., Stanley, P., Anumah, P., Onyekperem, C., Boah, E. 2020. "Computational fluid dynamics for ameliorating oil recovery using silicon-based nanofluids and ethanol in oil-wet reservoirs". Energy Reports, 6, 3023-3035.

[9] Daccord, G., Lenormand, R., Lietard, O. 1993. "Chemical Dissolution of a Porous Medium by a Reactive Fluid—I. Model for the Wormholing" Phenomenon. Chem. Eng. Sci. 48(1), 169-178.

[10] Economides, M. J., Hill, A. D., Ehlig-Economides, C. 2008. "Petroleum Production Systems". PTR Prentice Hall, 1994.

[11] Afgan, I., Moulinec, C., Laurence. D. 2008. "Numerical simulation of generic side mirror of a car using large eddy simulation with polyhedral meshes". International journal for numerical methods in fluids 56 (8), 1107-1113.

[12] Filippone, A., Afgan, I. 2008. "Orthogonal blade-vortex interaction on a helicopter tail rotor". AIAA journal 46 (6), 1476-1489.

[13] Guleren, K. M., Afgan, I., Turan. A. 2010. "Predictions of turbulent flow for the impeller of a NASA low-speed centrifugal compressor". Journal of Turbomachinery 132 (2).

[14] Han, X., Sagaut, P., Lucor, D., Afgan, I. 2012. "Stochastic response of the laminar flow past a flat plate under uncertain inflow conditions". International Journal of Computational Fluid Dynamics 26 (2), 101-117.

[15] McNaughton, J., Rolfo, S., Apsley, D., Afgan, I., Stansby, P., Stallard, T. 2012. "CFD prediction of turbulent flow on an experimental tidal stream turbine using RANS modelling". 1st Asian Wave and Tidal Energy Conference, Jeju Island, Korea, 2012, Power 1 (2), 0-3.

[16] Afgan, I., Benhamadouche, S., Han, X., Sagaut, P., Laurence, D. 2013. "Flow over a flat plate with uniform inlet and incident coherent gusts". Journal of Fluid Mechanics 720, 457-485.

[17] Ahmed, U., Afgan, I., Apsley, D., Stallard, T., Stansby, P. 2015. "CFD simulations of a full-scale tidal turbine: comparison of les and rans with field data". 11th European Wave and Tidal Energy Conference.

[18] Wu, Z., Laurence, D., Afgan, I. 2017. "Direct numerical simulation of a low momentum round jet in channel crossflow". Nuclear Engineering and Design 313, 273-284.

[19] Wu, Z., Laurence, D., Iacovides, H., Afgan, I. 2017. "Direct simulation of conjugate heat transfer of jet in channel crossflow". International Journal of Heat and Mass Transfer 110, 193-208.

[20] Abed, N., Afgan, I. 2017. "A CFD study of flow quantities and heat transfer by changing a vertical to diameter ratio and horizontal to diameter ratio in inline tube banks using URANS turbulence models". International Communications in Heat and Mass Transfer 89, 18-30.

[21] Kahil, Y., Benhamadouche, S., Berrouk, A. S., Afgan, I. 2019. "Simulation of subcritical-Reynolds-number flow around four cylinders in square arrangement configuration using LES". European Journal of Mechanics-B/Fluids 74, 111-122.

[22] Wu, Z., Laurence, D., Utyuzhnikov, S., Afgan, I. 2019. "Proper orthogonal decomposition and dynamic mode decomposition of jet in channel crossflow". Nuclear Engineering and Design 344, 54-68.

[23] Nguyen, PTL, Uribe, J. C., Afgan, I., Laurence, D. 2019. “A dual-grid hybrid RANS/LES model for under-resolved near-wall regions and its application to heated and separating flows”. Flow, Turbulence and Combustion, 1-25.
[24] Benhamadouche, S., Afgan, I., Manceau, R. 2020. “Numerical simulations of flow and heat transfer in a wall-bounded pin matrix”. Flow, Turbulence and Combustion 104 (1), 19-44.
[25] Abed, N., Afgan, I., Cioncolini, A., Iacovides H., Nasser, A. 2020. “Assessment and evaluation of the thermal performance of various working fluids in parabolic trough collectors of solar thermal power plants under non-uniform heat flux”. Energies 13 (15), 3776.
[26] Revell, A., Afgan, I., Ali, A., Santasmasas, M., Craft, T., de Rosis, A., Holgate, J. “Coupled hybrid RANS-LES research at the university of Manchester”. ERCOFTAC Bulletin 120, 67.
[27] Abed, N., Afgan, I. 2020. “An extensive review of various technologies for enhancing the thermal and optical performances of parabolic trough collectors”. International Journal of Energy Research 44 (7), 5117-5164.
[28] Abed, N., Afgan, I., Cioncolini, A., Iacovides, H., Nasser, A., Mekhail, T. 2020. “Thermal performance evaluation of various nanofluids with non-uniform heating for parabolic trough collectors”. Case Studies in Thermal Engineering 22, 100769.
[29] Ahmed, U., Apsley, D., Stallard, T., Stansby, P., Afgan, I. 2021. “Turbulent length scales and budgets of Reynolds stress-transport for open-channel flows; friction Reynolds numbers Re_τ = 150, 400 and 1020”. Journal of Hydraulic Research 59 (1), 36-50.
[30] Abed, N., Afgan, I., Iacovides, H., Cioncolini, A., Khurshid, I., Nasser, A. 2021. “Thermal-Hydraulic Analysis of Parabolic Trough Collectors Using Straight Conical Strip Inserts with Nanofluids”. Nanomaterials 11 (4), 853.
[31] Ali, A. E. A., Afgan, I., Laurence, D., Revell, A. 2021. “A dual-mesh hybrid RANS-LES simulation of the buoyant flow in a differentially heated square cavity with an improved resolution criterion”. Computers & Fluids 224, 104949.
[32] Hung, K. M., Hill, A. D., Sepehrnoori, K. A. 1989. “Mechanistic Model of Wormhole Growth in Carbonate Matrix Acidizing and Acid Fracturing”. SPE J. Petrol. Techn. 41(1), 59-66.
[33] Fredd, C. N., Fogler, H. S. 1998. “Influence of Transport and Reaction on Wormhole Formation in Porous Media”. AIChE J. 44, 1933–1949.
[34] Kalia, N., Balakotaiah, V. 2007. “Modeling and Analysis of Wormhole Formation in Reactive Dissolution of Carbonate Rocks”. Chem. Eng. Sci. 62, 919–928.
[35] Babaei, M., Sedighi, M. 2018. “Impact of Phase Saturation on Wormhole Formation in Rock Matrix Acidizing”. Chem. Eng. Sci. 177, 39-52.
[36] Dong, K., Zhu, D., Hill, A. D. 2018. “Mechanism of Wormholing and Its Optimal Conditions: a Fundamental Explanation”. J. Petrol. Sci. Eng. 169, 126–134.
[37] Buijse, M. A., Glasbergen, G. 2005. “A Semiempirical Model to Calculate Wormhole Growth in Carbonate Acidizing”. Paper SPE 96892, SPE Annual Technical Conference and Exhibition, Dallas, Texas, USA.
[38] Furui, K., Burton, R. C., Burkhead, D. W., Abdelmalek, N. A., Hill, A. D., Zhu, D., Nozaki, M. 2012. “A Comprehensive Model of High-Rate Matrix-Acid Stimulation for Long Horizontal Wells in Carbonate Reservoirs: Part I-Scaling Up Core-Level Acid Wormholing to Field Treatments”. SPE J. 17(1) 271-279.
[39] Ali, M. T., Nasr-El-Din, H. A. 2019. “A Robust Model to Simulate Dolomite-Matrix Acidizing”. SPE Prod & Oper 34, 109–129.
[40] Ali, M. T., Nasr-El-Din, H. A. 2020. “New Insights into Carbonate Matrix Acidizing Treatments: A Mathematical and Experimental Study”. SPE J. 25, 1272–1284.
[41] Abdollahi, R., Shadizadeh, S. R., Zargar, G. 2014. “Experimental Investigation of Acid-Induced Sludge Precipitation Using Acid Additives in Iran”. Energ. Sourc. Part A 36, 1793-1799.
[42] Tabzar, A., Fathinasab, M., Salehi, A., Bahrami, B., Mohammadi, A. H. 2018. “Multiphase flow modeling of asphaltene precipitation and deposition”. Oil Gas Sci. Technol. Rev. IFP Energies nouvelles, 73, 51.
[43] Shukla, S., Zhu, D., Hill, A. D. 2006. “The Effect of Phase Saturation Conditions on Wormhole Propagation in Carbonate Acidizing”. SPE J. 11. 273–281.
[44] Liu, M., Zhang, S., Mou, J., Zhou, F. 2013. “Wormhole Propagation Behavior under Reservoir Condition in Carbonate Acidizing. Transp”. Porous Med. 96, 203–220.

[45] Ghommem, M., Zhao, W., Dyer, S., Qiu, X., Brady, D. 2015. "Carbonate Acidizing: Modeling, Analysis, and Characterization of Wormhole Formation and Propagation". J. Petrol. Sci. Eng. 131, 18-33.
[46] Houchin, L. R., Dunlap, D. D., Arnold, B. D., Domke, K. M. 1990. "The Occurrence and Control of Acid-induced Asphaltene sludge". Paper SPE 19419, SPE Formation Damage Control Symposium, Lafayette, Louisiana, USA, 1990.
[47] Kumar, R., He, J., Nasr-El-Din, H. 2014. "New Insights on the Effect of Oil Saturation on the Optimal Acid-Injection Rate in Carbonate Acidizing". Paper SPE 169134, SPE Improved Oil Recovery Symposium, Tulsa, Oklahoma, USA.
[48] AlMubarak, T., AlKhaldi, M., AlMubarak, M., Rafie, M., Al-Ibrahim, H., AlBokhari, N. 2015. "Investigation of Acid-Induced Emulsion and Asphaltene Precipitation in Low Permeability Carbonate Reservoirs". Paper SPE 178034, SPE Saudi Arabia Section Annual Technical Symposium and Exhibition, Al-Khobar, Saudi Arabia.
[49] Rietjens, M., Van Haasterecht, M. 2003. "Phase Transport of HCl, HFeCl4, Water, and Crude Oil Components in Acid–Crude Oil Systems". J. Collo. Interf. Sci. 268 (2), 489-500.
[50] Alrashidi, H., Ibrahim, A. F., Nasr-El-Din, H. A. 2018. "Bio-Oil Dispersants Effectiveness on Asphaltene Sludge During Carbonate Acidizing Treatment". Paper SPE 191165, SPE Trinidad and Tobago Section Energy Resources Conference, Port of Spain, Trinidad and Tobago.
[51] Civan, F. 2016. "Reservoir Formation Damage Fundamentals, Modeling, Assessment, and Mitigation". Third edition, Gulf Publishing Company, Houston, Texas.
[52] Mullins, O. C., Sheu, E. Y., Hammam, I. A., Marshall, A. G. 2007. "Asphaltenes, Heavy Oils, and Petroelomics". Springer, New York City, USA.
[53] Yonebayashi, H., Al Mutairi, A. M., Al Habshi, A. M., Urasaki, D. 2011. "Dynamic Asphaltene Behavior for Gas-Injection Risk Analysis". SPE Reser. Evalu. Eng. J. 14 (4), 493-504.
[54] Gruesbeck, C., Collins, R. E. 1982. "Entrainment of Deposition of Fine particles in Porous media". SPE J. 22 (6) (1982), 847–856.
[55] Wang, S., Civan, F. 2001. "Productivity decline of vertical and horizontal wells by asphaltene deposition in petroleum reservoirs". Paper SPE 64991, SPE International Symposium on Oilfield chemistry, Houston, Texas, USA.
[56] Mehana, M., Abraham, J., Fahes, M. 2019. "The Impact of Asphaltene Deposition on Fluid Flow in Sandstone". J. Petrol. Sci. Eng. 174, 676-681.
[57] Afra, S., Samouei, H., Golshahi, N., Nasr-El-Din, H. 2020. "Alterations of Asphaltene Chemical structure due to Carbon dioxide Injection". Fuel 272, 117708.
[58] Soulgani, S. B.,Tohidi, B., Ahmadi, J. M., Rashtchian, D. 2011. "Modeling Formation Damage due to Asphaltene Deposition in the Porous Media". Energy & Fuels 25, 753-761.
[59] Almehaideb, R. A. 2004. "Asphaltene Precipitation and Deposition in the near wellbore region: a modeling approach". J. Pet. Sci. Eng. 42, 157-170.
[60] Yaseen, S., Mansoori, G. A. 2018. "Asphaltene Aggregation due to Waterflooding (A Molecular Dynamics Study)". J. Petro. Sci. Eng. 170, 177-183.
[61] Khurshid, I., Choe, J. 2018. "Analysis of Thermal Disturbance and Formation damage during CO_2 Injection in shallow and deep reservoirs". Int. J. Oil Gas Coal Techn. 11(2), 141-153.
[62] Khurshid, I., Al-Shalabi, E. W., Al-Attar, H., Al-Neaimi, A. K. 2020. "Analysis of Formation Damage and Fracture Choking in Hydraulically Induced Fractured Reservoirs due to Asphaltene Deposition". Journal of Petroleum Exploration and Production Technology, 173.
[63] Bagheri, M. B., Kharrat, R., Ghotby, C. 2011. "Experimental Investigation of the Asphaltene Deposition Process during Different Production Schemes". Oil Gas Sci. Techn. 66(3), 507-519.

601
602
603
604

605

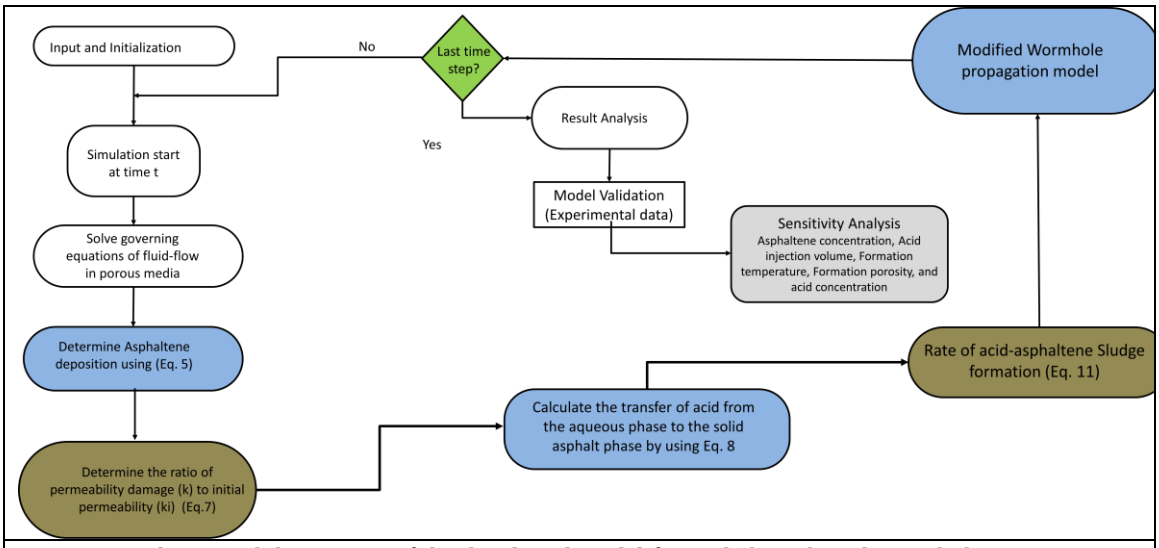

Fig. 2 Mathematical description of the developed model for asphaltene based wormhole penetration modeling

606
607
608
609

610
611

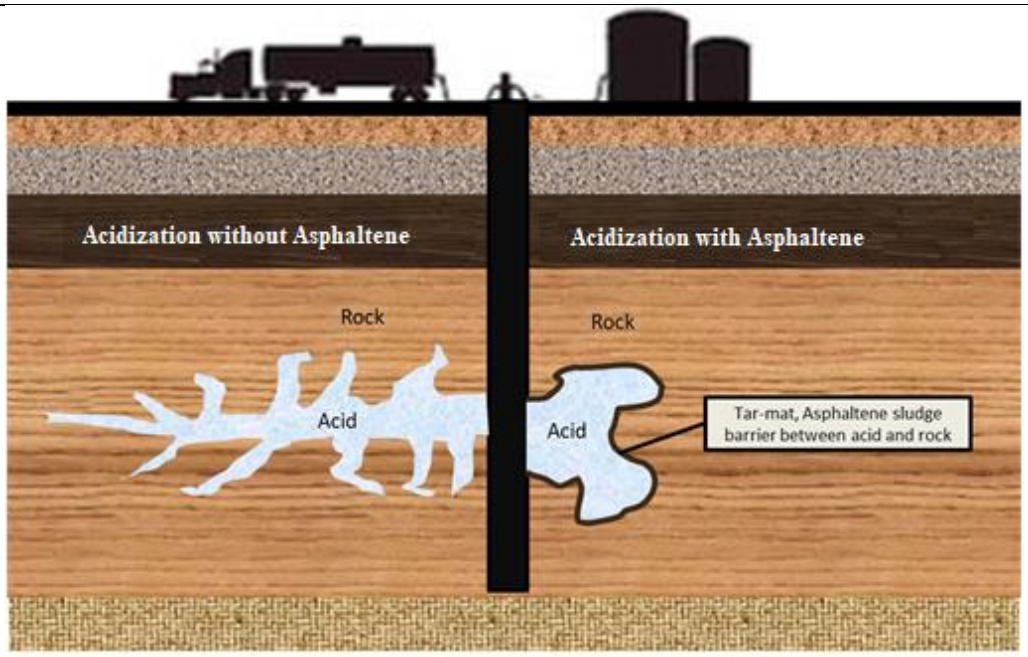

Fig. 3 Schematic of matrix acidization with and without asphaltene

612
613
614

615

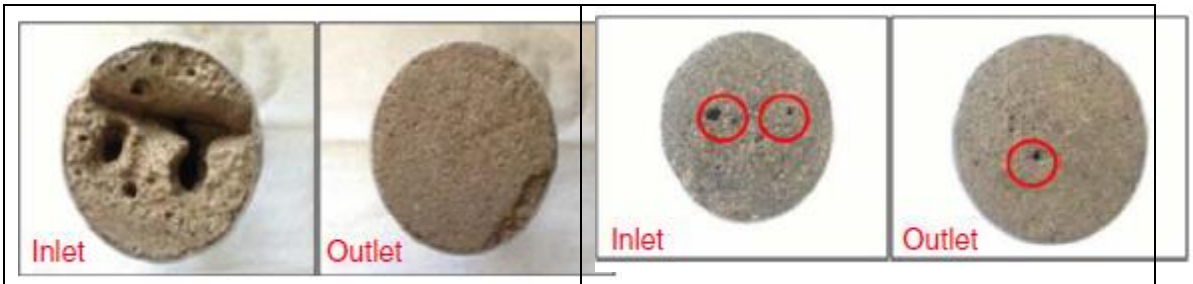

i. Brine saturated core ii. Residual oil saturated core

Fig. 4 Comparison of inlet and outlet faces of the 6-inch limestone cores with 15 wt. % HCl injection at $5 \times 10^{-7} m^3/min$ and 93.3 ºC [25]

616
617

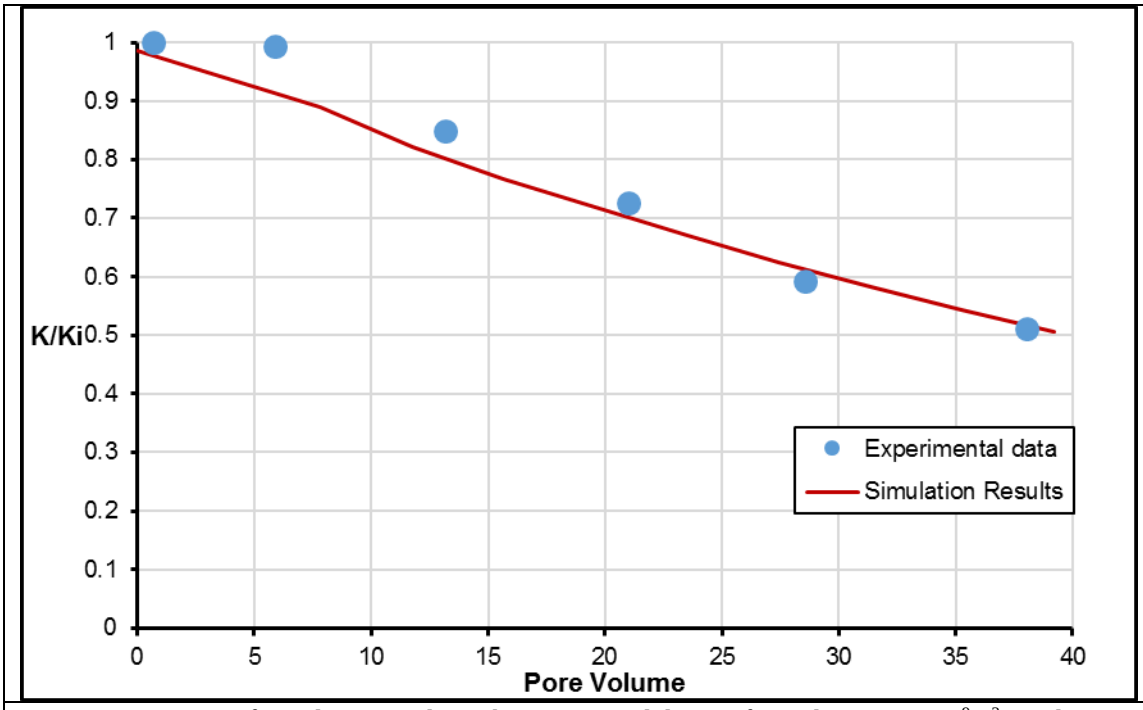

Fig. 5 Comparison of simulation results with experimental data perfomred at $2.76 \times 10^{-9} m^3/s$ and 80 ºC [36]

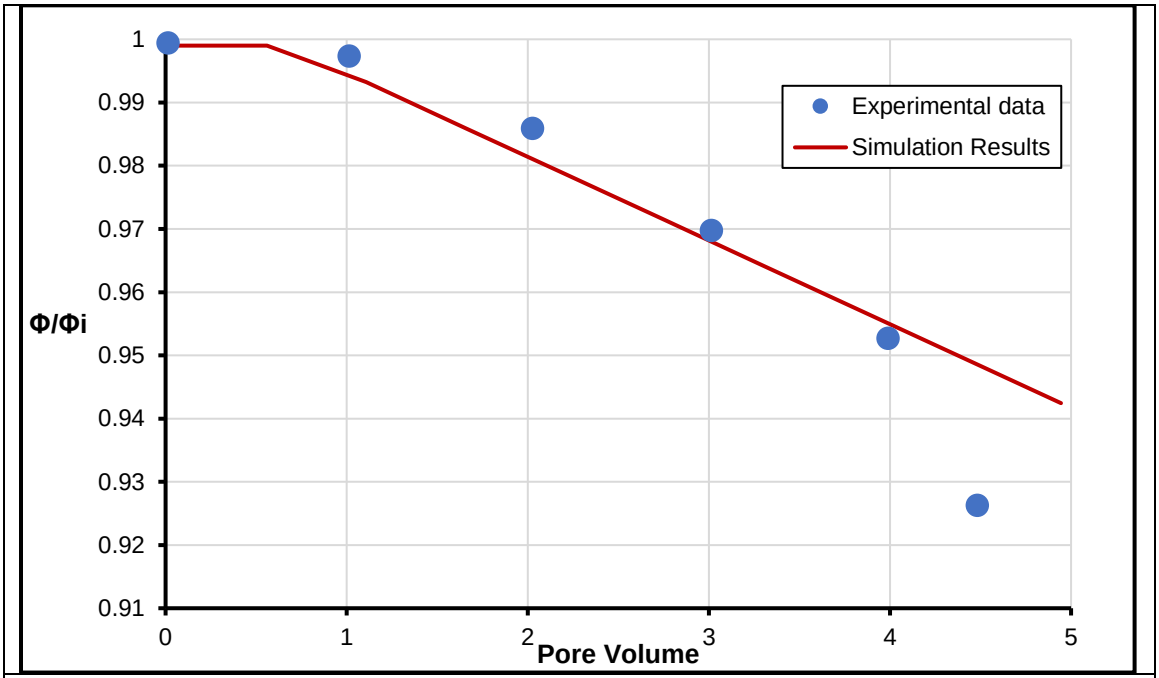

Fig. 6 Comparison of results with experimental data perfomred at $1.33 \times 10^{-8} m^3/s$ and 96 ºC [41]

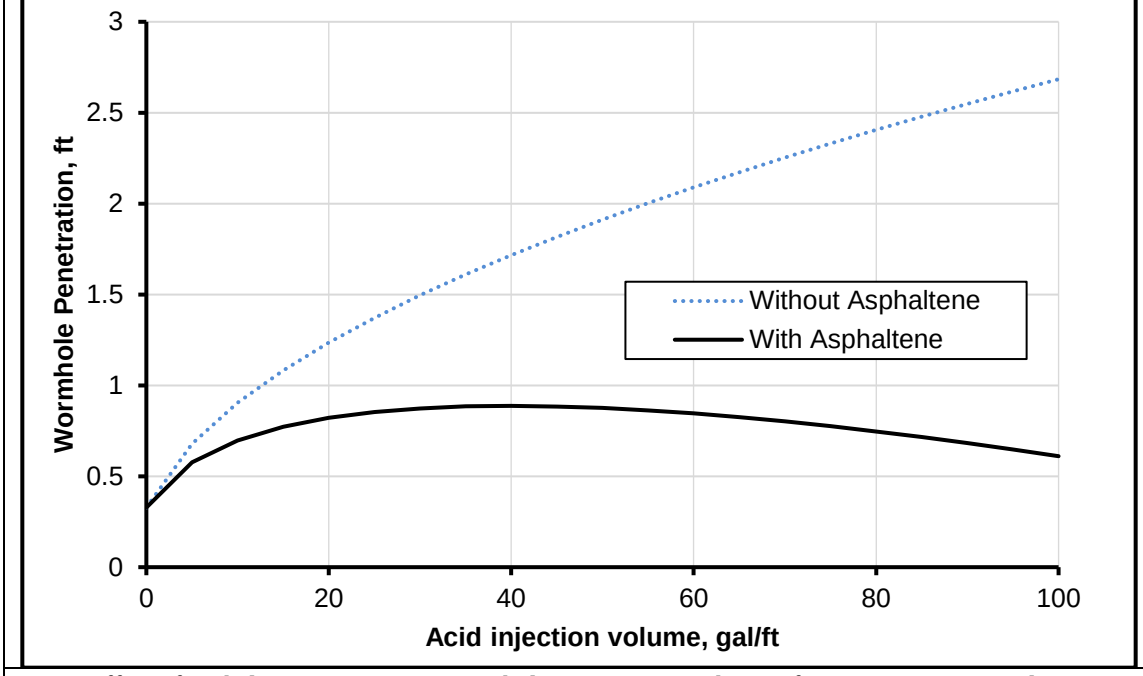

Fig. 7 Effect of asphaltene presence on wormhole penetration with 30% formation porosity and 15 wt. % acid concentration

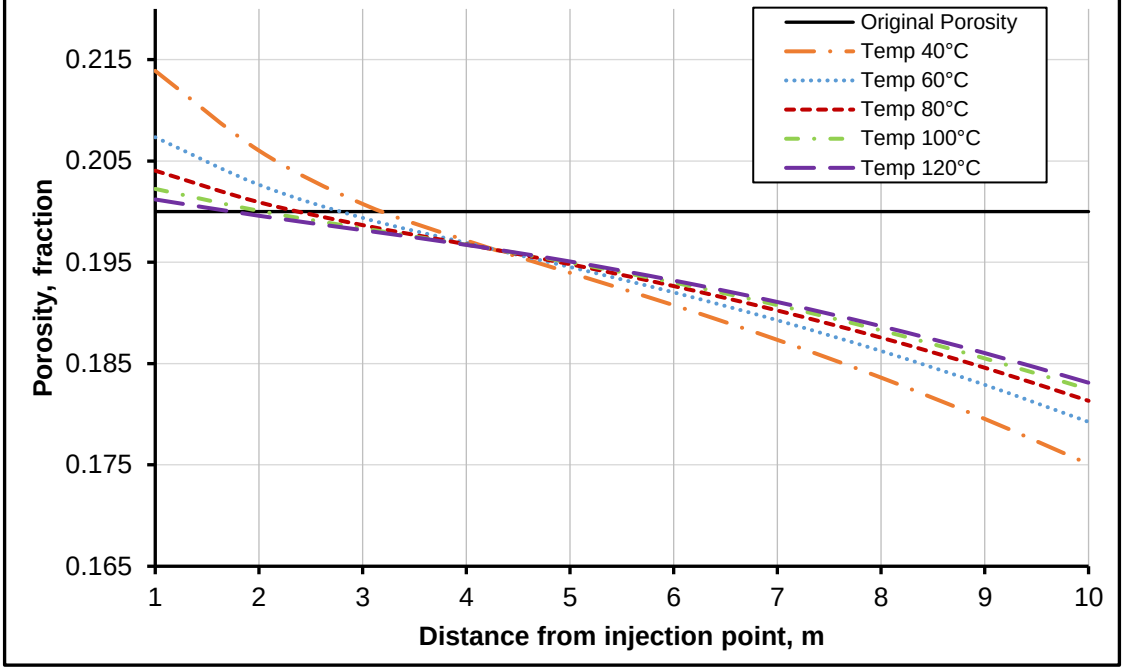

Fig. 8 Effect of temperature on wormhole penetration in the presence of 5.3 wt. % asphaltene and 30% formation porosity

631

632

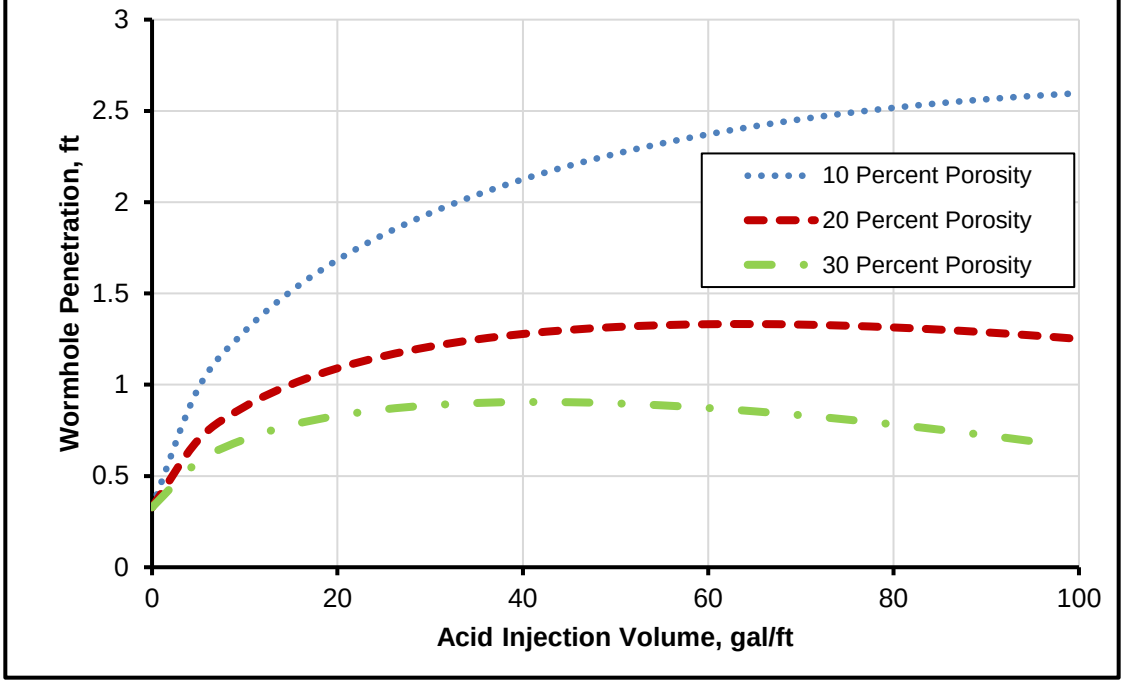

Fig. 9 Effect of formation porosity on wormholing in the presence of 5.3 wt. % asphaltene and 15 wt. % acid concentration

633
634

635

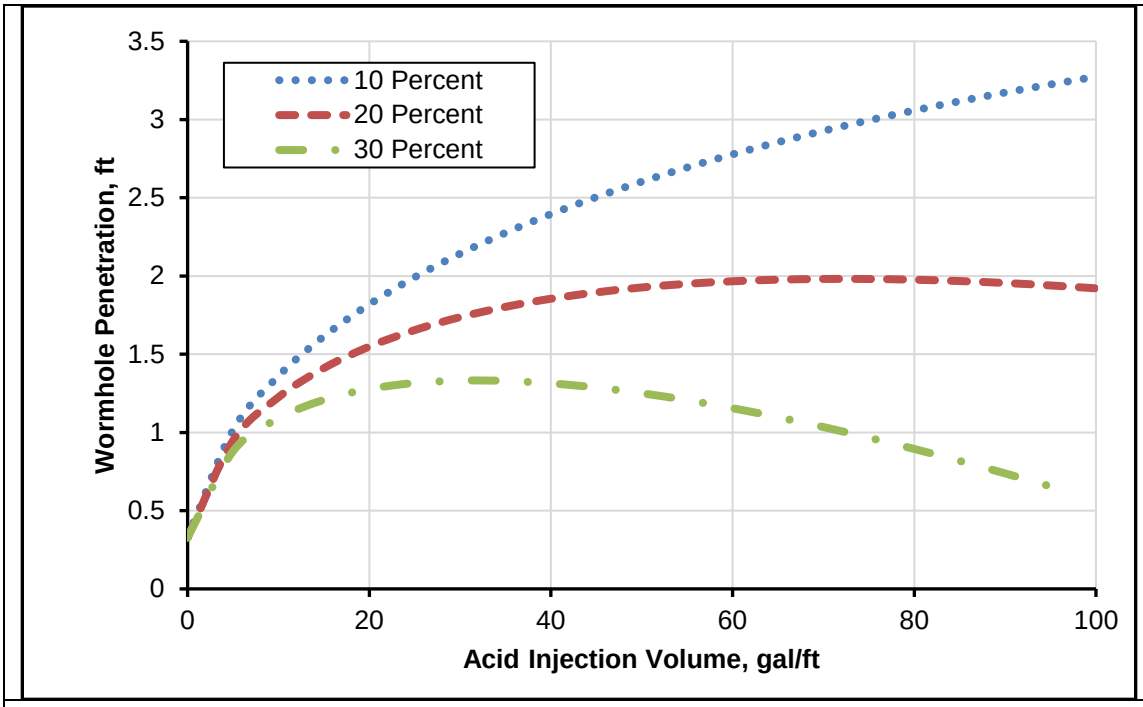

Fig. 10 Effect of acid concentration on wormholing with 30% formation porosity and 5.3 wt. % asphaltene

636
637

638

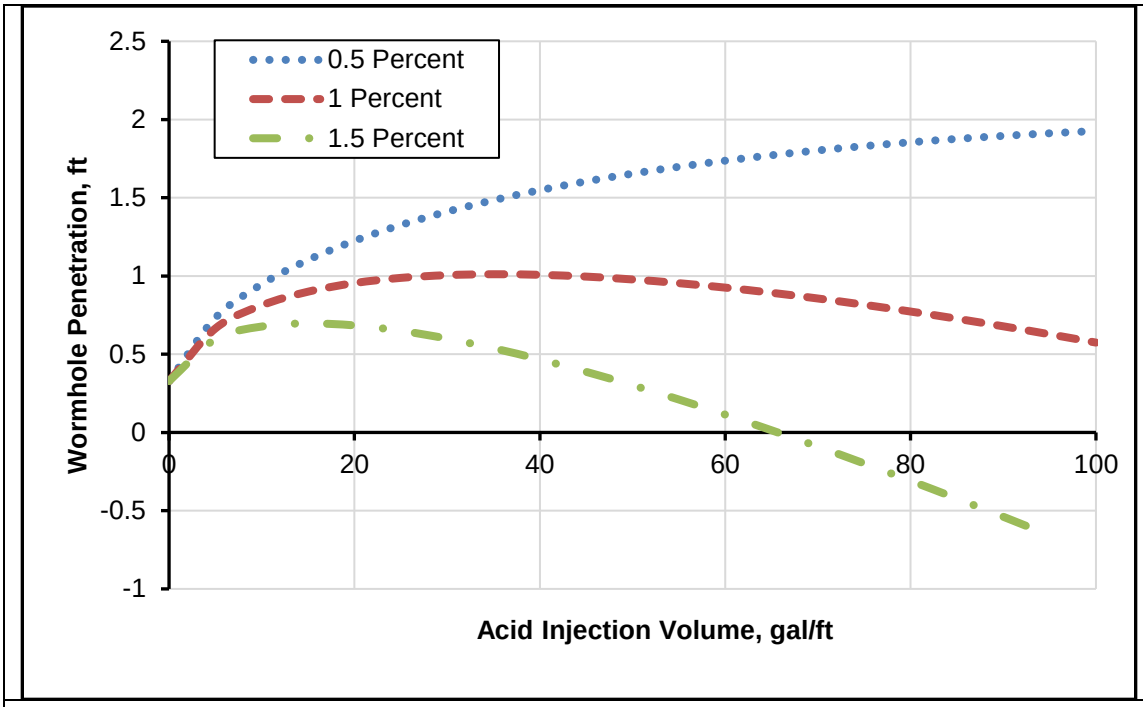

Fig. 11 Effect of asphaltene concentration on wormholing with 30% formation porosity and 15 wt. % acid concentration

639
640

641

642 **Table 1 Summary of the input parameters used in the Acid-Asphaltene formation reaction**

Parameter	Value
Formation Porosity (ϕ), percent	30
Wellbore Radius (r), cm	9.998
Acid Density (ρ), g/cm^3	1.07
Acid Concentration (C_a), % weight	15
Acid Capacity Number (N_c)	0.035
Rock Density (ρ), g/cm^3	2.71
Rock Wormholing Efficiency (τ)	0.0711
Reservoir Thickness (h), m	30.49
Asphaltene Concentration (C_{as}), % weight	5.3
Asphaltene Reaction Rate Coefficient (χ)	4.65×10^{-3}
Asphaltene Entrainment Rate Coefficient (β)	0.6

643

644